

# Dispersion Polymerization of Methyl Methacrylate in Supercritical Carbon Dioxide: An Investigation into Stabilizer Anchor Group

Helen M. Woods,<sup>†,‡</sup> Cécile Nouvel,<sup>†,§</sup> Peter Licence,<sup>†,||</sup> Derek J. Irvine,<sup>⊥,‡</sup> and Steven M. Howdle<sup>\*,†</sup>

School of Chemistry, The University of Nottingham, University Park, Nottingham, NG7 2RD, U.K., and Uniqema R&D Department, Wilton Research Centre, PO Box 90, Middlesbrough, Cleveland, TS90 8JE, U.K.

Received August 2, 2004; Revised Manuscript Received February 1, 2005

**ABSTRACT:** New stabilizers for the dispersion polymerization of methyl methacrylate (MMA) in supercritical carbon dioxide (scCO<sub>2</sub>) were prepared and studied in terms of their anchor group architecture. The same perfluoropolyether (PFPE) chain was used in each case as the CO<sub>2</sub>-philic portion of the stabilizer and four different PMMA-philic headgroups were investigated as anchoring units: an alcohol, an acetate group, a methacrylate unit, and a PMMA block. When compared to the stabilizing ability of PFPE-alcohol, incorporation of an anchor group as small as an acetate group, or a reactive group such as a methacrylate unit, was found to have a dramatic effect upon the dispersion polymerization of MMA in scCO<sub>2</sub>. Their incorporation led to a significant increase in PMMA yield and molecular weight and an improvement of the morphology of the polymer product. A method for the synthesis of PFPE-*b*-PMMA diblock copolymers is reported via atom transfer radical polymerization (ATRP) from a PFPE-bromoester macroinitiator in a fluorinated solvent (pentafluorobutane). This method allows the controlled synthesis of PFPE-*b*-PMMA diblock copolymers with well-defined architecture. These copolymers were found to be effective stabilizers in scCO<sub>2</sub>, leading to excellent PMMA yield with high molecular weight and a fine morphology. The effect of PFPE and PMMA block length on the copolymer stabilizing ability was also studied to probe the influence of the stabilizer anchor-soluble balance (ASB). In addition, the phase behavior of each stabilizer in CO<sub>2</sub> or a mixture of CO<sub>2</sub>/MMA was studied to elucidate the effect of stabilizer structure on CO<sub>2</sub>-philicity and stabilizing ability.

## 1. Introduction

Supercritical carbon dioxide (scCO<sub>2</sub>) is a benign medium that has shown great potential as a replacement for conventional organic solvents.<sup>1,2</sup> Over the past decade it has been investigated as a solvent for a variety of chemical processes such as polymerization and materials processing,<sup>3–7</sup> catalysis,<sup>8,9</sup> and extraction.<sup>1,10–12</sup> There are many advantages associated with the use of CO<sub>2</sub> as a reaction or processing solvent, including lack of toxic solvent residues, low cost, easily accessible critical point, and tunable solvent power. However, CO<sub>2</sub> is a poor solvent for high molecular weight compounds, with the exception of amorphous or low-melting fluoropolymers and silicones.<sup>13,14</sup> As a result, processes in scCO<sub>2</sub> often require the aid of a surfactant to ensure dispersion of the desired solute in the continuous phase.<sup>3–5,15–19</sup>

Highly CO<sub>2</sub>-phobic polymers such as poly(methyl methacrylate) (PMMA) can be synthesized in scCO<sub>2</sub> by dispersion polymerization using a surfactant.<sup>3–5,20–23</sup> The surfactant partitions between the continuous and polymer phases and prevents aggregation of the growing polymer particles through a steric stabilization mechanism. Without the use of a surfactant, low molecular weight polymer is obtained in poor yield with a nondescript morphology.

DeSimone et al. reported the first dispersion polymerization of methyl methacrylate (MMA) in scCO<sub>2</sub> using an amorphous fluoropolymer (poly(dihydroperfluorooctyl acrylate), PFOA) as the stabilizer.<sup>20</sup> This material consists of a PMMA-philic backbone, which interacts with the growing PMMA particles, and fluorinated CO<sub>2</sub>-philic grafts, which extend into the CO<sub>2</sub> phase. Since this work, a number of other stabilizer architectures based on block<sup>22,24–28</sup> and graft<sup>23,29</sup> copolymers have been described. A reactive macromonomer surfactant has also been reported<sup>30–36</sup> (poly(dimethylsiloxane) (PDMS) monomethacrylate), which acts as a stabilizer by chemically reacting with the growing polymer chains during the polymerization. The drawback to the use of this type of stabilizer is that it is ultimately incorporated in the final polymer product. A commercially available, acid terminated perfluoropolyether (PFPE) stabilizer (Krytox 157 FSL, Dupont) that anchors to PMMA chains by a reversible hydrogen bonding interaction has also been reported.<sup>37,38</sup> The lack of C–H bonds along the PFPE backbone prevents hydrogen abstraction and chemical incorporation of the stabilizer into the polymer product. Derivatizing Krytox 157 FSL with an ester group also leads to an effective stabilizer which is thought to interact with the PMMA particles through a weak van der Waals interaction.<sup>39</sup>

To date there have been a limited number of studies into the effect of surfactant architecture on stabilizing ability. Canelas et al. investigated the anchor-soluble balance (ASB—ratio of polymer-philic to CO<sub>2</sub>-philic portions in a surfactant) of the diblock stabilizer polystyrene(PS)-*b*-PDMS, which was used successfully to stabilize dispersion polymerizations of styrene in scCO<sub>2</sub>.<sup>25</sup> Increasing the length of the PS anchor portion

\* Corresponding author. E-mail: Steve.Howdle@nottingham.ac.uk. Telephone: +44(0)115 951 3486. Fax: +44(0)115 951 3058.

<sup>†</sup> The University of Nottingham.

<sup>‡</sup> E-mail: Pcxhwmw@nottingham.ac.uk.

<sup>§</sup> E-mail: Cecile.Nouvel@ensic.inpl-nancy.fr.

<sup>||</sup> E-mail: Pete.Licence@nottingham.ac.uk.

<sup>⊥</sup> E-mail: Derek.Irvine@uniqema.com.

<sup>⊥</sup> Wilton Research Centre.

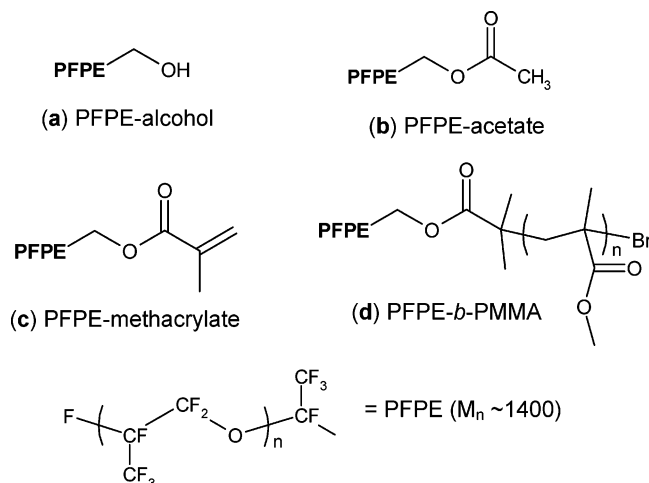


**Figure 1.** Stabilizer materials investigated in terms of their anchoring ability. Each consists of a different anchoring headgroup, (a) an alcohol group, (b) an acetate group, (c) a methacrylate unit, and (d) a PMMA block, but the same PFPE tail ( $M_n \sim 1400$  g/mol), which acts as the  $\text{CO}_2$ -philic portion.

(i.e., increasing the ASB of the stabilizer) led to larger, more monodisperse colloidal particles although no trend was observed in the molecular weight and yield of the polymer product. A strong dependence on ASB was also observed by Lepilleur and Beckman who investigated the molecular architecture of a fluorinated graft stabilizer for the dispersion polymerization of MMA in  $\text{scCO}_2$ .<sup>29</sup> They found that increasing the ASB of the stabilizer (increasing the length of the anchor portion) led to improved polymerization rates and products. However, a point was reached where the different portions of the stabilizer weighed too heavily toward the anchoring component, making the stabilizer insoluble in the continuous phase and drastically reducing its stabilizing ability. This clearly emphasizes the necessity for balance between the soluble ( $\text{CO}_2$ -philic) and anchoring (polymer-philic) groups within a stabilizer.

In this study, stabilizers with very different anchoring groups were examined for use in dispersion polymerizations of MMA in  $\text{scCO}_2$ . Four PMMA-philic headgroups were investigated as anchoring units: an alcohol group, an acetate group, a methacrylate unit, and a PMMA block (Figure 1a–d). These different anchor groups were combined with an identical  $\text{CO}_2$ -philic PFPE chain (Figure 1,  $M_n \sim 1400$ ) allowing their individual anchoring ability to be investigated. For the PMMA capped stabilizer, the influence of PFPE-*b*-PMMA ASB was further investigated by varying the length of both the  $\text{CO}_2$ -soluble PFPE portion and the PMMA anchoring block. The phase behavior of all the stabilizers was studied in  $\text{CO}_2$  or a mixture of  $\text{CO}_2$ /MMA using a newly developed hydraulic variable volume view cell.<sup>40</sup> The phase behavior data provide information about the compatibility of each stabiliser with  $\text{CO}_2$  and the temperature/pressure conditions under which initial polymerization mixtures ( $\text{CO}_2$ /MMA/stabilizer) are completely homogeneous.

## 2. Experimental Section

**Materials.** Monohydroxyl terminated PFPEs (Krytox alcohols,  $M_n \sim 1400$ , 1750, 4780 g/mol, Dupont) were used as received. Toluene was dried over an aluminum oxide tower under an inert atmosphere before use.  $\alpha$ -Bromoisobutyryl bromide (98%, Aldrich), methacryloyl chloride (97%, with 200 ppm methylhydroquinone as stabilizer, Aldrich) acetyl chloride

(98.5%, Aldrich), triethylamine (99%, Fischer Scientific) and 1,1,2-trichloroethane (Aldrich, 99%) were all used as received. MMA (99%, with 10–100 ppm monomethyl ether hydroquinone as inhibitor, Aldrich) and 1,1,1,3,3-pentafluorobutane ( $\text{BuF}_5$ , Solkane 365 MFC, Solvay) were dried over  $\text{CaH}_2$ , distilled under reduced pressure and stored under an inert atmosphere before use. 2,2'-bipyridine (bipy, 99%) and copper(I) chloride (99%, Aldrich) were used as received. SFC grade, high-purity carbon dioxide (BOC gases) was used as received. The initiator 2,2'-azobis(isobutyronitrile) (AIBN, 98%, Acros) was re-crystallized from THF before use.

**Characterization.**  $^1\text{H}$  NMR spectra were recorded in  $\text{CDCl}_3$  on a Bruker DPX-300 using protio impurities of the deuterated solvent as a reference for  $^1\text{H}$  shifts. Gel permeation chromatography (GPC) was performed in  $\text{CHCl}_3$  using a Polymer Labs LC1120 HPLC pump, two PLgel 5  $\mu\text{m}$  Mixed-D separation columns and an evaporative light scattering detector (Polymer Labs PL-ELS 1000). Both sample analysis and calibration were conducted at a flow rate of 1 mL/min. Calibration was achieved by means of polystyrene narrow standards (EasiCal PS2, Polymer Labs). For GPC analysis of the diblock PFPE-*b*-PMMA copolymers PMMA standards (EasiCal PMMA1, Polymer Labs) were used. Scanning electron microscopy (SEM) images were obtained using a Phillips 505 spectrometer. Samples were mounted on aluminum stubs using adhesive carbon tabs and sputter coated with gold before analysis. Mean particle diameter ( $D_n$ ,  $\mu\text{m}$ ) was determined by measuring the diameter of  $\sim 100$  particles and taking a mean of these data. The coefficient of variance (CV), an indication of particle size distribution, was then established using the equation  $\text{CV} = (\sigma/D_n) \times 100$ , where  $\sigma$  = standard deviation of particle diameter ( $\mu\text{m}$ ).<sup>41</sup>

**Synthesis of PFPE–Acetate and PFPE–Methacrylate Stabilizers and PFPE–Bromoester Macroinitiator.** For the synthesis of PFPE–acetate, PFPE–alcohol ( $M_n \sim 1400$ , 5 g, 3.6 mmol) was first dried by azeotropic distillation from toluene ( $\sim 20$  mL). The dry PFPE was then dissolved in 25 mL of 1,1,2-trichloroethane. Triethylamine (0.76 mL, 5.4 mmol) was added to the reaction mixture under nitrogen, followed by slow addition of acetyl chloride (0.39 mL, 5.4 mmol). The reaction was left to proceed for 48 h at  $40^\circ\text{C}$  with stirring, and the modified PFPE was then recovered by pouring the reaction mixture into methanol. The polymer product was washed with methanol several times before removal of residual solvent under reduced pressure at room temperature. The same synthetic method was adopted for the synthesis of PFPE–methacrylate and PFPE–bromoester. For these reactions, toluene was used as the reaction solvent (25 mL) and methacryloyl chloride (0.53 mL, 5.4 mmol) and  $\alpha$ -bromoisobutyryl bromide (0.67 mL, 5.4 mmol) were used as the respective acid chloride and acid bromide end-capping reagents. For each reaction, complete conversion of the PFPE–alcohol end groups was observed by  $^1\text{H}$  NMR. Calculations were made by comparing the signal for the methylene group protons at the end of the PFPE chain (m, 2H, 4.2–4.8 ppm) with the signal for the methyl group protons of the new anchor headgroup (acetate, s, 3H, 1.85 ppm; methacrylate, s, 3H, 1.8–1.9 ppm; bromoester, s, 6H, 1.7–1.8 ppm).

**Synthesis of PFPE-*b*-PMMA Stabilizers by ATRP.** In a typical reaction, the PFPE–bromoester macroinitiator (e.g.,  $M_n \sim 1550$ , 10.0 g, 6.5 mmol) was dried by azeotropic distillation from toluene (20 mL).  $\text{Cu}^+\text{Cl}$  (0.64 g, 6.5 mmol) and the bipy ligand (2.05 g, 13 mmol) were then added to the dry PFPE–bromoester initiator under a flow of nitrogen. The reactants were dissolved in  $\text{BuF}_5$  (23 mL, [PFPE–bromoester] = 0.19 mol/L), to yield a brown solution, although the copper catalyst appeared insoluble in this solvent. MMA monomer was degassed with nitrogen for 30 min and the desired amount transferred to the reaction mixture by capillary under nitrogen (11.3 mL, [MMA] = 3.1 mol/L). The reaction mixture turned green over time due to the formation of  $\text{Cu}(\text{II})$ . Samples (1 mL) taken from the reaction flask at regular time intervals were purified by dissolution in THF, filtered over a silica column (to remove the copper catalyst) and precipitated in hexane; each was then analyzed by  $^1\text{H}$  NMR. Copolymers made from

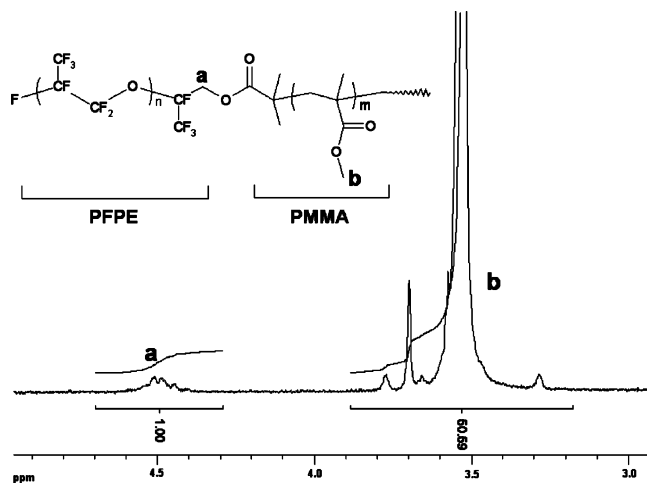


**Figure 2.**  $^1\text{H}$  NMR spectrum for PFPE-*b*-PMMA showing comparison of the signal for the methylene protons at the end of the PFPE chain (a) and the signal for the methyl ester protons of the PMMA block (b). The relative integrals of these peaks allow calculation of the PMMA block length.

the highest molecular weight PFPE ( $M_n \sim 4700$  g/mol) were purified by several reprecipitations in methanol.

Monomer conversion was determined by  $^1\text{H}$  NMR analysis of the unpurified 1 mL samples. This was calculated by comparing the signal for the methyl ester protons of the PMMA block (m, 3H, 3.6 ppm) with the signal for the methyl ester group of unreacted MMA (s, 3H, 3.7 ppm). To determine the degree of polymerization,  $^1\text{H}$  NMR spectra were recorded for the purified samples and comparison was made between the signal for the methyl ester protons of the PMMA block (m, 3H, 3.57 ppm) and the signal for the methylene protons at the end of the PFPE chain (n, 2H, 4.5–4.7 ppm—see Figure 2). A typical  $^1\text{H}$  NMR spectrum of the purified product revealed 4 peaks:  $\delta_{\text{H}} = 4.5\text{--}4.7$  ppm (2H,  $\text{CH}_2$  of PFPE); 3.57 ppm (3H,  $\text{CH}_3\text{COO}$ —, in PMMA repetitive unit); 1.7–2.1 ppm (2H,  $\text{CH}_2$  of PMMA repetitive unit and 6H,  $\text{CH}_3$  of PFPE–bromoester end group); and 0.7–1.2 ppm (3H,  $\text{CH}_3\text{--C--COOCH}_3$  of PMMA repeat unit).

**Dispersion Polymerizations of MMA in  $\text{scCO}_2$  Using PFPE End-Capped Stabilizers.** Polymerizations in  $\text{scCO}_2$  were performed in a 60 mL stainless steel, clamp sealed autoclave equipped with a magnetically coupled overhead stirrer and a pressure relief valve.<sup>42</sup> Heating was provided by a heating jacket, which was controlled by a digital controller (CAL instruments). The temperature inside the autoclave was monitored using a thermocouple in contact with the  $\text{scCO}_2$  (RS components). In a typical polymerization, the autoclave was charged with reactants (10 g MMA, 0.1 g AIBN, 1–3 wt % stabilizer with respect to monomer) and then pressurized to  $\sim 3500$  psi ( $\sim 24$  MPa) with high-grade nitrogen. This procedure was designed to leak test the equipment and to degas the reaction system. Following careful release of nitrogen, the autoclave was filled with  $\text{CO}_2$  and heated to the desired reaction temperature (65  $^\circ\text{C}$ ). Once this temperature was reached, additional  $\text{CO}_2$  was added to a pressure of  $\sim 3200$ – $3500$  psi ( $\sim 22$ – $24$  MPa). A gentle stirring rate (approximately 100 rpm) was provided when filling the autoclave to ensure effective mixing of the reactants; however, stirring was halted once the desired reaction conditions had been reached. Previous work has shown that dispersion polymerizations in  $\text{scCO}_2$  stabilized by an acid terminated PFPE (Krytox 157 FSL, Dupont) become unstable at a surprisingly moderate stirring rate (above 25 rpm)<sup>43</sup> and for this reason the reactions reported here were not stirred for the duration. The reaction was allowed to proceed for 5 h, after which time the heating was stopped and the autoclave allowed to cool to room temperature. The  $\text{CO}_2$  was then slowly vented. The rate of venting was found to have no effect on the morphology of the final product.

In a successful polymerization, the polymer product was recovered as a dry, white powder. Monomer conversion was

measured gravimetrically, molecular weight ( $M_w$ ) and polydispersity (PDI) were obtained by GPC (e.g., Table 2) and product morphology was examined by SEM (e.g., Figure 4). Without adequate stabilization, a mixture of monomer, oil, and hard clear solid was retrieved from the reaction vessel. With a successful stabilizer, the product PMMA was recovered as a dry, free-flowing white powder. In all cases, solid product was retrieved for SEM and GPC analysis. To ensure accurate measurement of PMMA yield, the remaining material was dissolved in THF, reprecipitated in hexane and dried under reduced pressure. This procedure requires significant amounts of organic solvents and would not be considered as an environmentally responsible method. However, for the purposes of this research it allows the most accurate determination and comparison of polymer yield and therefore stabilizer ability.

**Solubility Measurements.** Solubility measurements were performed using a newly developed hydraulic variable volume view cell<sup>40</sup> consisting of a static front sapphire window and a moveable rear sapphire piston in contact with a hydraulic ram. The entire contents of the cell are easily observed through the large aperture sapphire windows. In a typical experiment, a known weight of stabilizer or stabilizer/MMA was added to the view cell along with a magnetic stirrer bar.  $\text{CO}_2$  was passed into the cell using a weighed, high-pressure, stainless steel bomb. After addition of the  $\text{CO}_2$ , the bomb was reweighed in order to calculate the exact composition of the stabilizer/ $\text{CO}_2$  or stabilizer/MMA/ $\text{CO}_2$  mixture. This was recorded in weight percent (wt %) using the following equations: wt % stabilizer = (mass of stabilizer(g)/[mass of stabilizer(g) + mass of  $\text{CO}_2$ (g)]) and wt % MMA = (mass of MMA(g)/[mass of MMA(g) + mass of  $\text{CO}_2$ (g)]). The cell was heated to a given temperature and the contents allowed to equilibrate with stirring. The pressure, and therefore density, of the  $\text{scCO}_2$  was then increased by slowly reducing the volume of the cell until a single homogeneous phase was observed. The cloud point pressure of the mixture was recorded by slowly increasing the volume, and hence decreasing the pressure of the  $\text{CO}_2$ , until the dissolved stabilizer began to precipitate out of solution; this led to the mixture turning cloudy. The cloud point was taken as the point at which it was no longer possible to see the rear of the cell. This process was repeated three times and an average of the results taken as the cloud point pressure. Cloud point pressures were recorded at various temperatures between 25 and 85  $^\circ\text{C}$  (for example measurements see Figures 5 and 7). The maximum pressure rating of the cell used was 6000 psi (41.4 MPa).

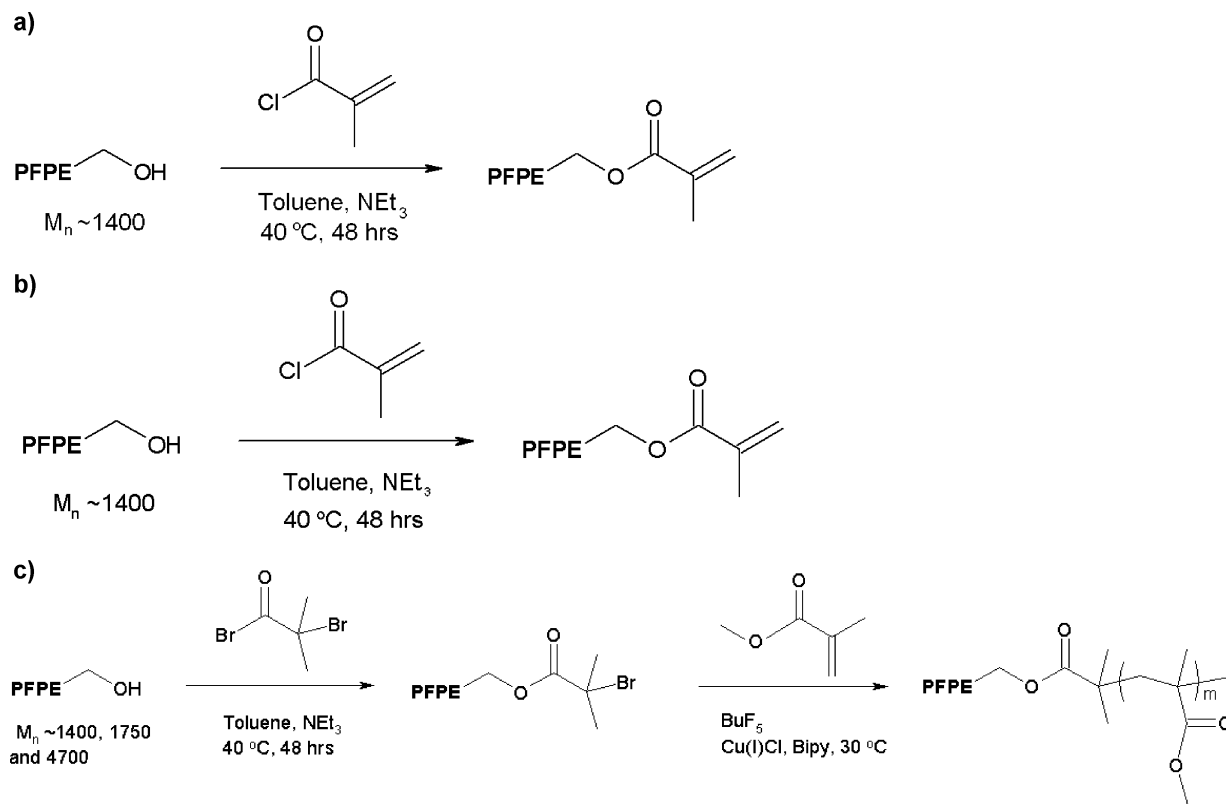
### 3. Results and Discussion

**Synthesis of PFPE Based Stabilizers.** A  $\text{CO}_2$ -philic PFPE tail was modified with an acetate anchor group and a methacrylate anchor group by esterification reactions (Scheme 1, parts a and b). Each product was obtained in high yield ( $>90\%$ ). PFPE-*b*-PMMA diblock copolymers were prepared by a two-step synthesis as shown in Scheme 1c. First, PFPE–alcohol was modified to yield a terminal bromoester group. This PFPE–bromoester was then used as a macroinitiator for the controlled ATRP of MMA to form a PMMA block. Pentafluorobutane ( $\text{BuF}_5$ ) was chosen as the ATRP reaction solvent to ensure dissolution of the PFPE starting material as well as the MMA monomer and PMMA product. However, the catalyst  $\text{Cu}^{\text{I}}\text{Cl}$  was found to be insoluble in  $\text{BuF}_5$ , and the polymerization proceeded under heterogeneous conditions.

The kinetics of the ATRP reaction were investigated by taking samples from the reaction mixture at regular time intervals for analysis by  $^1\text{H}$  NMR. The polymerization was found to follow first-order kinetics with regards to monomer concentration as revealed by the linear increase of  $\ln([M]_0/[M])$  with time (Figure 3a). This indicates that the concentration of active radicals



Scheme 1

Table 1. Properties of the PFPE-*b*-PMMA Diblock Copolymers Synthesized by ATRP<sup>g</sup>

entry	diblock copolymer ( $M_n$ given in parens)	$M_n$ PFPE <sup>a</sup>	Cv (%) <sup>b</sup>	$M_n$ PMMA (theory) <sup>c</sup>	$M_n$ (NMR) <sup>d</sup>		$M_n$ total (GPC) <sup>e</sup>	PDI (GPC) <sup>e</sup>
					PMMA block	total		
1	PFPE(1750)- <i>b</i> -PMMA(2000)	1750	56	1300	2000	3750	6000	1.07
2	PFPE(1750)- <i>b</i> -PMMA(3300)	1750	74	1700	3300	5050	5300	1.12
3	PFPE(1750)- <i>b</i> -PMMA(5600)	1750	92	2200	5600	7350	9600	1.18
4	PFPE(4700)- <i>b</i> -PMMA(1700)	4700	41	1000	1800	6400	<i>f</i>	<i>f</i>
5	PFPE(1400)- <i>b</i> -PMMA(1900)	1400	87	900	1900	3400	2400	1.13
6	PFPE(1400)- <i>b</i> -PMMA(3500)	1400	88	1400	3500	4900	4800	1.26

<sup>a</sup> Supplied by Dupont, <sup>b</sup> Cv = monomer conversion, calculated from <sup>1</sup>H NMR, <sup>c</sup> ( $[M_0]/[I]$ ) × (Cv), <sup>d</sup> Determined by <sup>1</sup>H NMR, <sup>e</sup> Determined by GPC in CHCl<sub>3</sub> against PMMA standards, <sup>f</sup> Copolymer not soluble in CHCl<sub>3</sub>. <sup>g</sup> Entries 1–4 performed in BuF<sub>5</sub> at 30 °C, [MMA] ~4.5 mol/L; entry 5 performed in butanone at 40 °C, [MMA] 2.0 mol/L; entry 6 performed in toluene at 80 °C, [MMA] 3.0 mol/L. In each reaction initiator:Cu<sup>I</sup>Cl:bipy = 1:1:2 [initiator] = 0.19 mol/L.

Table 2. Polymerization Results for Different End-Capped PFPE ( $M_n$  ~1400) Stabilizers<sup>a</sup>

entry	stabilizer ( $M_n$ given in brackets)	mol % stab. wrt MMA	product morphology	yield (%)	$M_w$ (g/mol)	PDI
1	no stabilizer		monomer/oil	20	18 200	1.63
2	PFPE–alcohol(1400)	0.143	monomer/oil/clear solid	50	83 000	1.94
3	PFPE(1400)-acetate	0.139	white clumpy powder	83	216 600	1.42
4	PFPE(1400)-methacrylate	0.136	white powder	93	232 000	1.46
5	PFPE(1400)- <i>b</i> -PMMA(3500)	0.040	white powder	99	261 400	1.61
6*	PFPE–acid(2500)	0.040	white powder	96	171 000	1.56

<sup>a</sup> Polymerizations were carried out between 3200 and 3500 psi, at 65 °C and at a stabilizer loading of 2 wt % with respect to monomer and ~0.45 wt % with respect to CO<sub>2</sub>. Monomer loading = ~18 wt % with respect to CO<sub>2</sub>. Each experiment was repeated at least once and an average of the results taken. For comparison with the results shown here, entry 6 shows the result obtained when Krytox 157 FSL<sup>38</sup> is used as the stabilizer under the same conditions.

remained constant during the propagating stage. In addition, the molecular weight of the PMMA block was found to increase linearly with monomer conversion (Figure 3b). This observation, combined with the low polydispersity of the copolymer during chain growth, confirms that the polymerization proceeded under controlled conditions.<sup>44</sup>

The diblock copolymers obtained and their macromolecular parameters are summarized in Table 1. GPC

analysis revealed all products to have a narrow unimodal molecular weight distribution (PDI < 1.2, Figure 3a). The PMMA block molecular weight was not calculated from GPC data because the different solubility of the individual PMMA and PFPE blocks causes the hydrodynamic volume of each copolymer to be affected not only by molecular weight but also by the relative length of the fluorinated component. <sup>1</sup>H NMR analysis provides

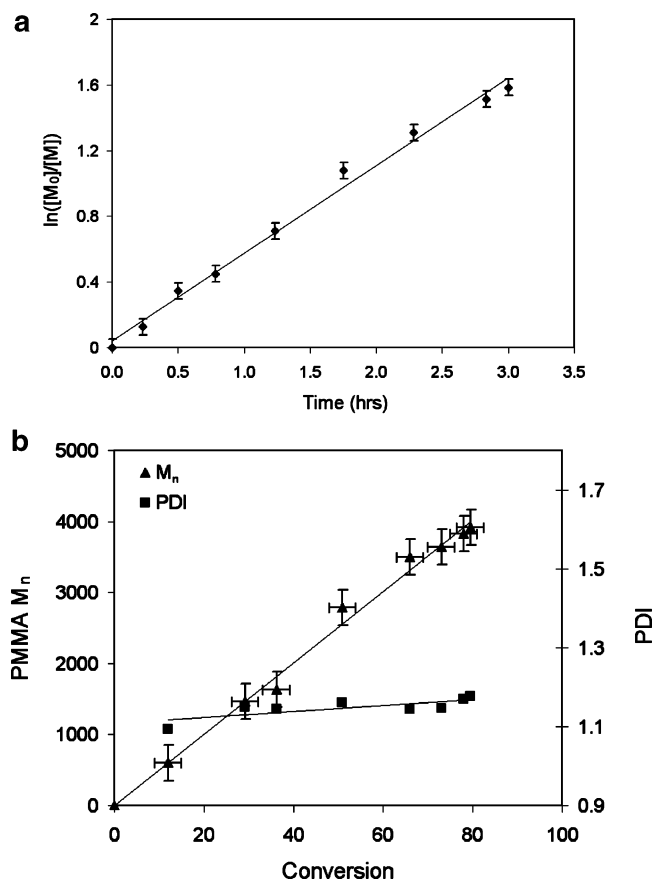


**Figure 3.** (a) First-order plot for the ATRP of MMA from a PFPE ( $M_n$  1750) macroinitiator. The linear progression indicates that the polymerization follows first-order kinetics with respect to monomer concentration and that the concentration of active radicals remained constant during the propagating stage. (b)  $M_n$  and PDI vs monomer conversion for the ATRP polymerization of MMA using PFPE( $M_n$  1750)-bromoester as a macroinitiator (Scheme 1c). The reaction was performed in  $\text{BuF}_5$  at 30 °C,  $[\text{MMA}] = 3.1 \text{ mol/L}$ , initiator: $\text{Cu}^{\text{I}}\text{Cl}:\text{bipy} = 1:1:2$ . Both PMMA  $M_n$  and monomer conversion were calculated by  $^1\text{H}$  NMR. PDI was determined by GPC in  $\text{CHCl}_3$  against PMMA narrow standards.

a more accurate estimate of the PMMA block length (see Table 1).

The PMMA blocks were found to be longer than theoretically calculated (Table 1, entries 1–4), which suggests that not all the initiator underwent reaction. This is likely a result of the poor solubility of the catalyst in the fluorinated solvent  $\text{BuF}_5$ , which limits its activity. Other solvents were tested, such as butanone (Table 1, entry 5) or toluene (entry 6), but did not promote any further control in the reaction. These solvents are both able to dissolve the catalyst complex but not the PFPE initiator; therefore, the reaction mixtures were again heterogeneous. A possible solution could be to adopt a fluorinated ligand to encourage dissolution of the  $\text{Cu}^{\text{I}}\text{Cl}$  catalyst in the fluorinated solvent. Alternatively, a hydrocarbon solvent combined with a fluorinated cosolvent could be used. This strategy was successful for Hems et al. in the synthesis of PMMA-*b*-poly(fluoroalkyl methacrylate) diblock copolymers,<sup>22</sup> but as yet we have not determined the correct solvent pairing for our diblock copolymers.

For the purposes of this research, the synthetic method adopted here allows the controlled synthesis of fluorinated diblock copolymers with narrow polydispersity. By quenching the ATRP after a certain reaction

time (established by kinetic studies, Figure 3) it was possible to obtain copolymers with varying PMMA block length for further investigation as stabilizers for the dispersion polymerization of MMA in  $\text{scCO}_2$ .

**Effect of PFPE Anchor Group on Stabilizing Ability.** End-capped materials, as well as the unmodified PFPE-alcohol, were tested as stabilizers in the dispersion polymerization of MMA in  $\text{scCO}_2$ . The effect of the surfactant anchor group on stabilizing activity was investigated in terms of PMMA yield, molecular weight and morphology. When no stabilizer was used, low molecular weight polymer was obtained in poor yield and in the form of a viscous oil (Table 2, entry 1). Addition of unmodified PFPE-alcohol to the reaction led to some improvement in yield and molecular weight, although the product was retrieved as a mixture of colorless solid and viscous oil (Table 2, entry 2). It is believed that the PFPE-alcohol anchors to the growing PMMA particles by a hydrogen bonding interaction. However, this material is likely to undergo a certain degree of self-association as a result of the hydroxyl end group,<sup>45</sup> which may prevent it from sufficiently anchoring to the PMMA. If the anchoring ability of a stabilizer is too weak, the equilibrium of the system favors unadsorbed single or associated stabilizer molecules in the continuous  $\text{CO}_2$  phase over adsorbed stabilizer at the polymer particle surface and as a result the stabilization is inefficient.<sup>46</sup>

When the same reaction was repeated in the presence of PFPE-acetate, there was a considerable improvement in PMMA yield and molecular weight (Table 2, entry 3), and the polymer product was retrieved as an agglomerated white powder. The acetate capped PFPE apparently interacts with the growing polymer more effectively through a weak van der Waals interaction with PMMA<sup>39</sup> leading to improved stabilization compared to PFPE-alcohol. In addition, removal of the hydroxyl end group of the PFPE-alcohol is likely to reduce the degree of self-association between the PFPE chains<sup>45</sup> and therefore encourage better partitioning of the material into the polymer phase. The methacrylate capped PFPE led to high PMMA yield and molecular weight, and the PMMA product was obtained in the form of a fluffy, white powder (Table 2, entry 4). In this case, it is possible for the stabilizer to covalently graft to the growing PMMA chains via the methacrylate end group. This would significantly enhance the ability of the PFPE to anchor to the growing polymer and may explain the observed improvement in the polymer product.  $^1\text{H}$  NMR analysis revealed that almost all the PFPE-methacrylate stabilizer remained in the PMMA product and this supports the idea that the stabilizer becomes chemically incorporated during dispersion polymerization. A PFPE-*b*-PMMA diblock copolymer, with a PMMA block  $\sim 3500 \text{ g/mol}$ , was found to be the most successful stabilizer at very low mol % concentration (Table 2, entry 5). A free-flowing, fine white powder was obtained in excellent yield and high molecular weight. There are two possible mechanisms by which the PFPE-*b*-PMMA copolymer interacts with the growing PMMA particles: it may graft onto the PMMA backbone through free radical hydrogen abstraction, or simply entangle with the growing polymer chains. Either of these interactions would enable the stabilizer to partition between the PMMA particles and the  $\text{CO}_2$  phase more effectively.

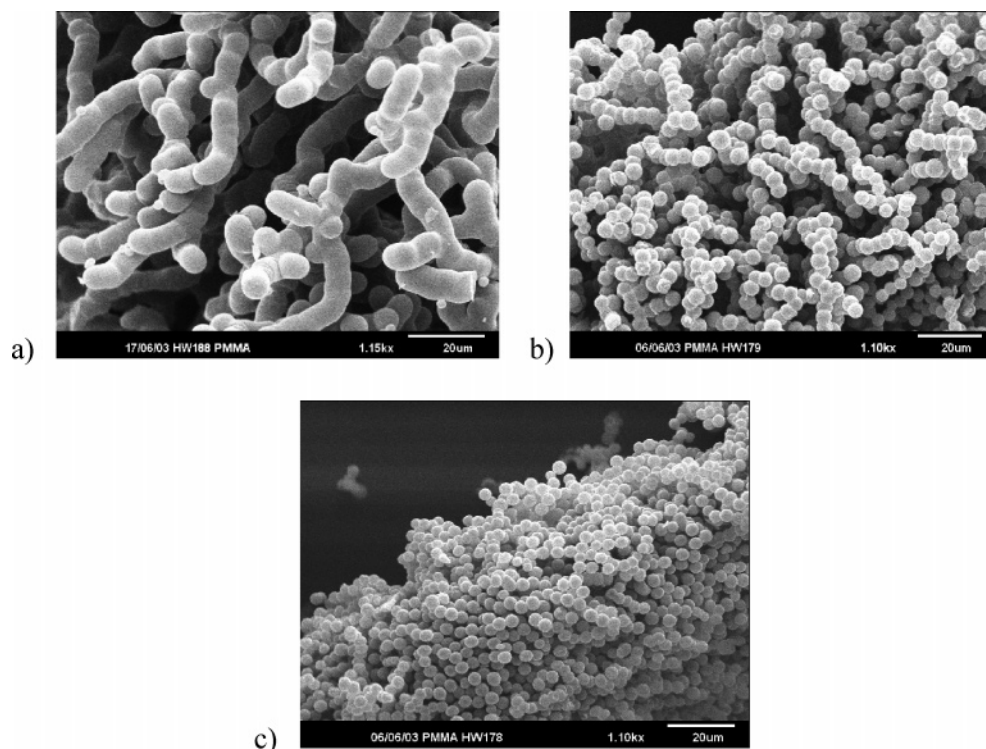


**Figure 4.** Effect of stabilizer anchor group on PMMA morphology: (a) PFP-acetate, agglomerated strings of particles; (b) PFPE-methacrylate, “pearl necklace” morphology,  $D_n = 5.0 \mu\text{m}$ ,  $\text{CV} = 8.6\%$ ; (c) PFPE-*b*-PMMA, discrete particles,  $D_n = 3.8 \mu\text{m}$ ,  $\text{CV} = 8.2\%$ .

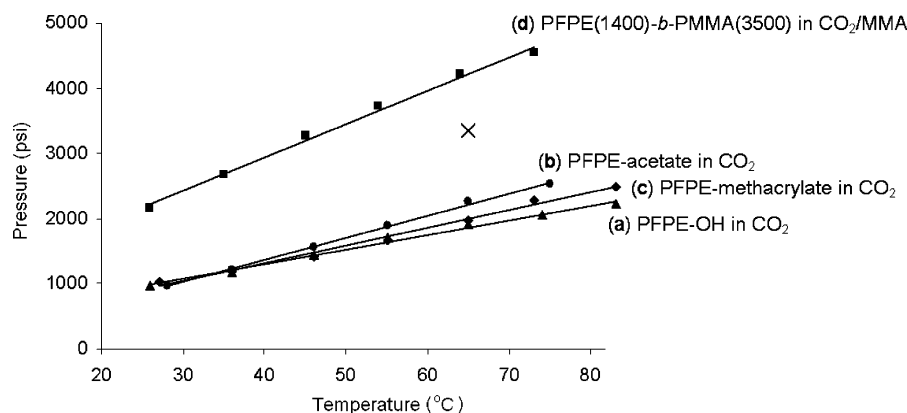


**Figure 5.** Solubility curves for PFPE stabilizers with different anchoring headgroups (a, b, and c recorded at 0.7 wt % polymer with respect to  $\text{CO}_2$ , d recorded at 0.4 wt % polymer and 18 wt % MMA with respect to  $\text{CO}_2$ ). The single cross indicates the conditions under which dispersion polymerizations were performed.

SEM micrographs of the different PMMA products were recorded to compare more accurately the effect of the different anchoring groups on the morphology of the polymer product (Figure 4). Agglomerated strings of particles were observed for the PMMA product stabilized by PFPE-acetate (Figure 4a), while a “pearl necklace” morphology can be seen for the PMMA product stabilized by PFPE-methacrylate (Figure 4b). Discrete particles were obtained when the diblock copolymer PFPE-*b*-PMMA was used, with a mean particle diameter of  $3.8 \mu\text{m}$  (Figure 4c) and a smaller particle size distribution (reduced coefficient of variance (CV)). These results indicate that anchoring group efficiency follows the trend PFPE-acetate < PFPE-methacrylate < PFPE-*b*-PMMA.

To investigate the effect of the anchoring headgroup on stabilizer  $\text{CO}_2$ -philicity, solubility curves were recorded for the different PFPE stabilizers in pure  $\text{CO}_2$ . PFPE-alcohol, PFPE-acetate, and PFPE-methacry-

late were each found to have excellent solubility in pure  $\text{CO}_2$  at the concentration used in a typical dispersion polymerization (0.4 wt % wrt  $\text{CO}_2$ ). In fact, at this loading cloud points were not observed for the end-capped polymers – instead bubble and dew points were recorded indicating the separation of  $\text{CO}_2$  gas or liquid from the homogeneous mixture. At a higher loading (0.7 wt %), the three stabilizers again exhibited very good solubility in  $\text{CO}_2$ , but in this case it was possible to measure cloud points for each of the polymers (curves a, b, and c in Figure 5). These data reveal PFPE-alcohol, PFPE-acetate, and PFPE-methacrylate to be completely soluble in pure  $\text{CO}_2$  under the conditions used in a dispersion polymerization reaction (65 °C and 3200–3500 psi, indicated by a single cross in Figure 5). End-capping the PFPE-alcohol with an acetate group or a methacrylate unit was found to have little effect on the overall solubility of the PFPE chain. This indicates that the differences observed in stabilizing



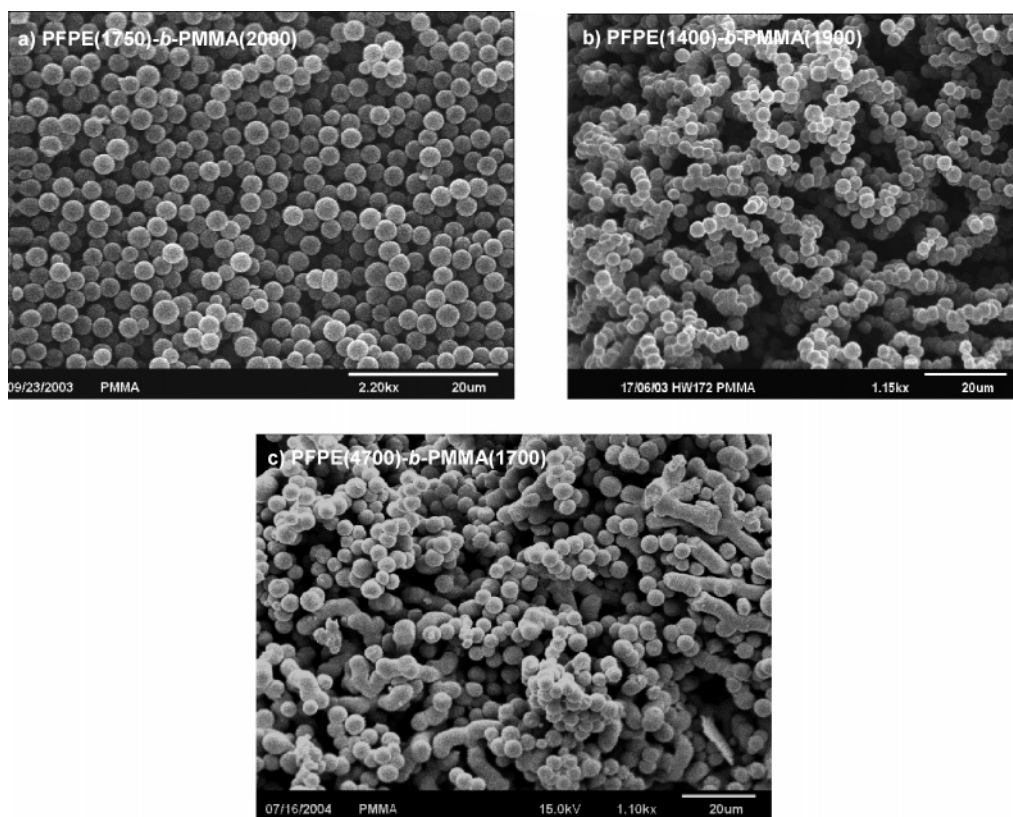


**Figure 6.** Effect of PFPE block length on PMMA product morphology. The PMMA block length of the stabilizer was kept constant at  $M_n \sim 2000$  g/mol. (a) PFPE(1750)-*b*-PMMA(2000), discrete particles,  $D_n = 2.9 \mu\text{m}$ , CV = 9.1%; (b) PFPE(1400)-*b*-PMMA(1900), some agglomeration,  $D_n = 3.4 \mu\text{m}$ , CV = 10.9%; (c) PFPE(4700)-*b*-PMMA(1700), some strings and agglomeration,  $D_n = 4.9 \mu\text{m}$ , CV = 18.0%.

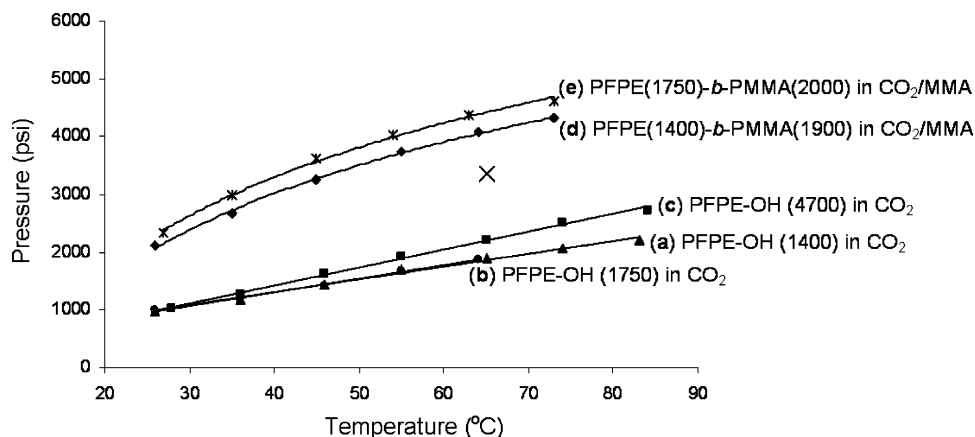


**Figure 7.** Solubility curves for PFPE-*b*-PMMA copolymers with different PFPE chain lengths but a similar length PMMA block ( $M_n \sim 2000$  g/mol). Curves a, b, and c were each recorded at 0.7 wt % polymer wrt CO<sub>2</sub>; curves d and e were recorded at 0.4 wt % polymer and 18 wt % MMA wrt CO<sub>2</sub>. The single cross indicates the conditions under which dispersion polymerizations were performed.

ability are a result of the different anchoring abilities of each of the headgroups and not a result of varying phase behavior in CO<sub>2</sub>.

Interestingly the most effective stabilizer, PFPE-*b*-PMMA, was found to be insoluble in pure CO<sub>2</sub> at a concentration of 0.4 wt % and within the pressure range of the apparatus used (maximum pressure rating 6000 psi). The PMMA block clearly reduces the solubility of the PFPE chain, which would be expected from the literature.<sup>14,45</sup> Mimicking the initial conditions of a polymerization reaction by adding MMA to the CO<sub>2</sub> (18 wt %) led to an improvement in the solubility of the copolymer and a solubility curve was measured (curve d, Figure 5). The MMA monomer clearly acts as a

cosolvent for the copolymer, enabling it to dissolve in the continuous phase at accessible pressures. This is a result of MMA providing enhanced interactions between the PMMA portion of the copolymer and the mixed CO<sub>2</sub>/MMA solvent.<sup>47</sup> When solubility measurements were recorded for PFPE-alcohol, PFPE-acetate, and PFPE-methacrylate with MMA monomer present the solubility of the materials at 0.7 wt % polymer and 18 wt % MMA did not significantly alter.

The PFPE-*b*-PMMA/MMA/CO<sub>2</sub> solubility curve reveals that under the conditions of a dispersion polymerization, not all the PFPE-*b*-PMMA stabilizer is dissolved in the reaction mixture. However, the miscibility pressures recorded in the view cell are not distinct

**Table 3. Dispersion Polymerization Results Obtained Using Various PFPE-*b*-PMMA Diblock Copolymers, and the Corresponding PFPE-Alcohol Starting Materials, as Stabilizers<sup>a</sup>**

entry	stabilizer ( $M_n$ given in parens)	ASB	mol % stab. wrt MMA	wt % stab. wrt CO <sub>2</sub>	yield (%)	$M_w$ (g/mol)	PDI	morphology	$D_n$ ( $\mu$ m)	CV (%)
1	PFPE-alcohol(1400)		0.143	~0.4	50	83 000	1.94	monomer/oil/ solid		
2	PFPE-alcohol(1750)		0.057	~0.2	46	88 700	2.11	monomer/oil/ solid		
3	PFPE-alcohol(4700)		0.021	~0.2	70	24 100	2.31	monomer/oil/solid		
4	PFPE(1400)- <i>b</i> -PMMA(1900)	1.4	0.038	~0.3	95	189 200	2.11	powder	3.4	10.9
5	PFPE(1750)- <i>b</i> -PMMA(2000)	1.1	0.040	~0.3	91	346 600	1.26	powder	2.9	9.1
6	PFPE(1750)- <i>b</i> -PMMA(3300)	1.9	0.040	~0.4	90	296 500	1.31	powder	1.4	21.6
7	PFPE(1750)- <i>b</i> -PMMA(5600)	3.2	0.038	~0.6	97	241 000	1.31	powder	1.8	33.7
8	PFPE(4700)- <i>b</i> -PMMA(1700)	0.4	0.040	~0.8	93	308 300	1.30	powder/some strings	4.9	18.0

<sup>a</sup> All polymerizations were carried out between 3200 and 3500 psi at 65 °C at a loading of ~18 wt % MMA with respect to CO<sub>2</sub>. Each experiment was repeated at least once and an average of the results taken. ASB =  $M_n$ PMMA/ $M_n$ PFPE

transitions, and it is therefore likely that a portion of the material will be dissolved in the continuous phase under the conditions of a reaction (most likely the lower molecular weight chains). It is perhaps this portion that acts to stabilize the dispersion of growing PMMA particles. The solubility information gained here draws us to some interesting conclusions. For example, the stabilizer does not have to be completely soluble in pure CO<sub>2</sub> but should be dispersed throughout the initial reaction mixture with the aid of MMA as a cosolvent. The ability of the stabilizer to partition is more important than it having very good overall solubility in CO<sub>2</sub>, hence it is essential that a stabilizer has very distinct CO<sub>2</sub>-philic and PMMA-philic portions within its architecture.

**Effect of ASB on the Stabilizing Ability of PFPE-*b*-PMMA Copolymers.** To further elucidate the role of the PFPE-*b*-PMMA stabilizer, various PFPE-*b*-PMMA diblock copolymers were synthesized with well-defined architectures and varying block length (Scheme 1c). The different block copolymer stabilizers are listed in Table 1 and the results obtained for the corresponding dispersion polymerizations are shown in Table 3.

Each PFPE-*b*-PMMA copolymer was found to act as a better stabilizer than the corresponding PFPE-alcohol (Table 3, entries 1–3), leading to high molecular weight PMMA in good yield and in the form of a free-flowing, white powder (entries 4–8). If copolymers with different PFPE chain lengths, but similar length PMMA blocks are compared, it can be seen that increasing the size of the PFPE portion from 1400 g/mol to 1750 g/mol substantially increases the molecular weight of the PMMA product, although product yield remains similar (Table 3, entries 4 and 5, PMMA block ~2000 g/mol).

Increasing the length of the PFPE tail further to 4700 g/mol leads to no additional improvement in the molecular weight of the product and the yield is again unaffected (Table 3, entry 8). SEM images of the PMMA products reveal that the particles stabilized by PFPE(1750)-*b*-PMMA(2000) are discrete and uniform in size (Figure 6a), whereas particles stabilized by PFPE(1400)-*b*-PMMA(1900) (Figure 6b) and PFPE(4700)-*b*-PMMA(1700) (Figure 6c) are larger and more agglomerated. PFPE-1750 therefore appears to be the most effective CO<sub>2</sub>-philic chain length when combined with a PMMA anchor block ~2000 g/mol. This stabilizer has an ASB ( $M_n$ PMMA/ $M_n$ PFPE) of 1.1, which represents the optimal balance between polymer-philic and CO<sub>2</sub>-philic portions for the stabilizers tested here.

The most important stage of a dispersion polymerization reaction is the nucleation stage when the growing polymer chains reach a critical molecular weight, become insoluble in the continuous phase and precipitate out of solution forming primary particles. This occurs

very early on in a polymerization, before ~0.1% conversion of the monomer.<sup>31–33,48</sup> At this point it is vital that stabilizer molecules are present in the continuous phase in order to quickly reach the particle surface and associate around the growing polymer. Therefore, it is beneficial to investigate the phase behavior of different stabilizers in the continuous phase of a polymerization reaction, to compare their stabilizing ability. The solubilities of PFPE(1400)-*b*-PMMA(1900), PFPE(1750)-*b*-PMMA(2000) and PFPE(4700)-*b*-PMMA(1700) were examined in pure CO<sub>2</sub> and a CO<sub>2</sub>/MMA mixture at the relative concentrations of a typical dispersion polymerization reaction (0.4 wt % stabilizer, 18 wt % MMA with respect to CO<sub>2</sub>). The solubility of the three unmodified PFPE-alcohols was also measured.

Each of the PFPE-alcohols was found to show good solubility in pure CO<sub>2</sub>. Miscibility pressures increased slightly with an increase in the molecular weight of the PFPE chain (see curves a, b, and c in Figure 7) as expected from the literature.<sup>49</sup> The PFPE-*b*-PMMA stabilizers were found to be insoluble in pure CO<sub>2</sub> up to the maximum pressure rating of the equipment used, despite each containing a highly CO<sub>2</sub>-philic PFPE portion. However, addition of MMA to the CO<sub>2</sub> led to a considerable improvement in the solubility of PFPE(1400)-*b*-PMMA(1900) and PFPE(1750)-*b*-PMMA(2000) (curves d and e in Figure 7), with PFPE(1400)-*b*-PMMA(1900) appearing slightly more soluble than PFPE(1750)-*b*-PMMA(2000) due to its higher molecular weight. The solubility curves reveal that both these copolymers are not completely dissolved under the temperature and pressure conditions of a typical dispersion polymerization reaction (indicated by a single cross in Figure 7). However, the miscibility pressure of each at 65 °C falls close to the pressure adopted in a polymerization and since the miscibility pressures recorded are not distinct transitions from a one-phase mixture to a two-phase mixture, a certain portion of each of these stabilizers is likely to be solubilized in the initial reaction mixture.

It is interesting that PFPE(1750)-*b*-PMMA(2000) was found to stabilize a more desirable PMMA product than that obtained using PFPE(1400)-*b*-PMMA(1900) (SEM images a and b Figure 6) despite PFPE(1400)-*b*-PMMA(1900) being marginally more soluble in the continuous phase (Figure 7). This highlights that in a dispersion polymerization, the requirement that a stabilizer demonstrates good solubility in the reaction mixture (CO<sub>2</sub>/MMA) is not the only essential property. It is also important that there is the correct balance between the anchor group and the soluble portion, promoting optimum partitioning of the stabilizer at the growing polymer surface. The fact that PFPE(1750)-*b*-PMMA(2000) is less soluble in the initial continuous phase may



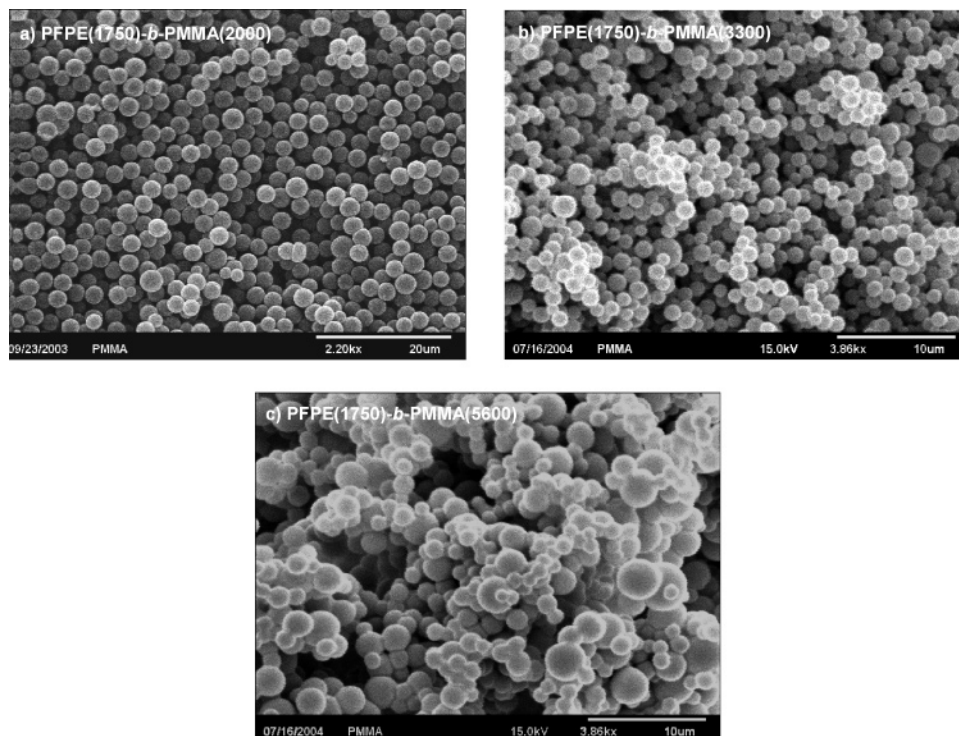


**Figure 8.** Effect of varying the stabilizer PMMA block length on product morphology. In this case the PFPE block length was kept constant at  $M_n \sim 1750$ . Key: (a) PFPE(1750)-*b*-PMMA(2000), discrete particles,  $D_n = 2.9 \mu\text{m}$ , CV = 9.1%; (b) PFPE(1750)-*b*-PMMA(3300), discrete particles,  $D_n = 1.4 \mu\text{m}$ , CV = 21.6%; (c) PFPE(1750)-*b*-PMMA(5600), range of particle sizes,  $D_n = 1.8 \mu\text{m}$ , CV = 33.7%.

act in its favor, since this might encourage the material to reside at the PMMA particle surface and partition between the PMMA and  $\text{CO}_2$  phases more effectively.

The PFPE(4700)-*b*-PMMA(1700) stabilizer did not completely dissolve in the  $\text{CO}_2$ /MMA system and a solubility curve could not be recorded. This observation may be a result of the copolymer having high molecular weight or containing some very high molecular weight fractions. Unfortunately, molecular weight data for this stabilizer could not be measured by GPC because of the poor solubility of the copolymer in  $\text{CH}_3\text{Cl}$ . Despite this, a certain portion of the copolymer did appear to be solubilized since the mixture turned cloudy when pressure inside the view cell was reduced from 6000 psi (i.e., when  $\text{CO}_2$  density was reduced). The more stabilizer dissolved in the reaction mixture the greater its efficiency at partitioning between the dispersed and continuous phases during nucleation.<sup>21</sup> Therefore, from the solubility results discussed above it is understandable that PFPE(1400)-*b*-PMMA(1900) and PFPE(1750)-*b*-PMMA(2000) act as more effective stabilizers than PFPE(4700)-*b*-PMMA(1700), as a greater proportion of the former two stabilizers is likely to be present in the continuous phase of a polymerization reaction.

It should be noted that due to the varying solubility of PFPE(1400)-*b*-PMMA(1900), PFPE(1750)-*b*-PMMA(2000), and PFPE(4700)-*b*-PMMA(1700) in the  $\text{CO}_2$ /MMA system, the concentration of each stabilizer under the initial conditions of a polymerization reaction will be different. To overcome this, polymerizations could be performed at higher  $\text{CO}_2$  pressure (for example  $\sim 5000$  psi) to encourage the concentration of stabilizer to be equal in the case of each copolymer. Here, our aim was to build on previous work regarding stabilizers that have been found to work very well at moderate  $\text{CO}_2$  pressures (e.g., Krytox 157 FSL<sup>38</sup>). A high reaction

pressure is commercially unappealing and energy inefficient, so it is advantageous to investigate stabilizers that perform well at lower pressure and to establish the reasons for their success in terms of their phase behavior under these conditions.

Copolymers with the same PFPE block length (PFPE-1750) but different PMMA block lengths were next compared. Increasing the size of the PMMA portion from 2000 to 5600 g/mol had little effect on product yield but led to a small decrease in PMMA molecular weight (Table 3, entries 5–7). SEM images (Figure 8) show that mean particle size decreases with increasing PMMA anchor group length, which is consistent with the work of Lepilleur et al., who noted a similar trend.<sup>29</sup> However, particle size distribution significantly rises as the size of the PMMA block is increased and this suggests that the efficiency of the stabilizer is compromised once the anchor group becomes greater than a certain molecular weight. The PMMA product stabilized by PFPE(1750)-*b*-PMMA(5600) (Figure 8c) also appears to be more agglomerated than the products stabilized by PFPE(1750)-*b*-PMMA(2000) and PFPE(1750)-*b*-PMMA(3300). It therefore seems that stabilizer efficiency follows the trend PFPE(1750)-*b*-PMMA(2000) > PFPE(1750)-*b*-PMMA(3300) > PFPE(1750)-*b*-PMMA(5600).

We had hoped to investigate the efficiency of a stabilizer with a smaller PMMA block ( $M_n < 2000$  g/mol) in order to find the minimum PMMA block length for successful stabilization. However, it proved difficult to make controlled blocks of PMMA shorter than  $\sim 15$  repeat units ( $M_n \sim 1500$  g/mol) by ATRP. It may be possible to achieve such block lengths, e.g. by early quenching of an ATRP reaction aimed at making a longer PMMA. Others may wish to explore this possibility, but it is outside the consideration of the work conducted here.

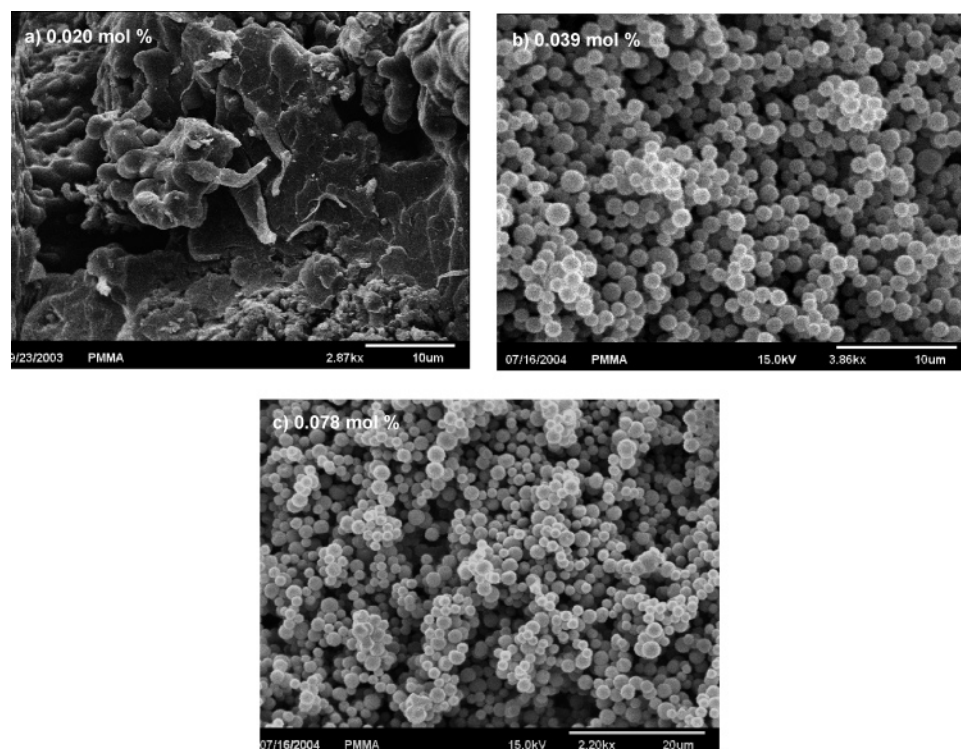


**Figure 9.** SEM images reveal the effect of PFPE(1750)-*b*-PMMA(3300) concentration on PMMA morphology. (a) 0.020 mol % with respect to monomer, sticky hard solid; (b) 0.039 mol %, discrete particles,  $D_n = 1.4 \mu\text{m}$ ,  $\text{CV} = 21.6\%$ ; (c) 0.078 mol %, discrete particles,  $D_n = 1.5 \mu\text{m}$ ,  $\text{CV} = 21.4\%$ .

**Table 4. Influence of Stabilizer Concentration on PMMA Product<sup>a</sup>**

entry	stabilizer	ASB	mol % stab. wrt mon.	wt % stab. wrt CO <sub>2</sub>	yield (%)	$M_w$ (g/mol)	PDI	product morphology	$D_n$ ( $\mu\text{m}$ )	CV (%)
1	PFPE(1750)- <i>b</i> -PMMA(2000)	1.1	0.019	~0.2	90	292 700	1.43	powder	3.6	12.3
2	PFPE(1750)- <i>b</i> -PMMA(2000)	1.1	0.039	~0.3	91	346 600	1.26	powder	2.8	9.1
3	PFPE(1750)- <i>b</i> -PMMA(3300)	1.9	0.020	~0.2	87	196 800	1.95	agglomerated particles		
4	PFPE(1750)- <i>b</i> -PMMA(3300)	1.9	0.039	~0.4	90	296 500	1.31	powder	1.4	21.6
5	PFPE(1750)- <i>b</i> -PMMA(3300)	1.9	0.078	~0.9	91	283 200	1.29	fine powder	1.5	21.4

<sup>a</sup> Two different PFPE-*b*-PMMA diblock copolymer stabilizers were investigated. All polymerizations carried out between 3200 and 3500 psi at 65 °C and at 18 wt % MMA with respect to CO<sub>2</sub>. Experiments were repeated at least once and an average of the results taken.

Solubility measurements revealed that PFPE(1750)-*b*-PMMA(2000) and PFPE(1750)-*b*-PMMA(3300) both have similar solubility in a CO<sub>2</sub>/MMA mixture at the relative concentrations of a polymerization reaction, with PFPE(1750)-*b*-PMMA(2000) showing slightly lower miscibility pressures. Most importantly, at 65 °C the miscibility pressure of each copolymer falls close to the pressure adopted in a polymerization, indicating that there will be a significant portion of each stabilizer dissolved in the initial reaction mixture. The copolymer PFPE(1750)-*b*-PMMA(5600) did not completely dissolve in a CO<sub>2</sub>/MMA mixture below 6000 psi pressure, revealing that the longer PMMA block compromises the overall solubility of the stabilizer in the polymerization reaction mixture. A reduction in stabilizer solubility ultimately reduces the amount of stabilizer available in the continuous phase to effectively partition at the particle surface during nucleation and this may explain why the PMMA product stabilized by PFPE(1750)-*b*-PMMA(5600) is more agglomerated (Figure 8c).

As a final point, it should be remembered that during a polymerization the concentration of MMA slowly drops as monomer is converted to polymer. Since MMA acts as a cosolvent for the PMMA capped stabilizers and aids their initial dissolution in the continuous CO<sub>2</sub> phase, a reduction in MMA concentration could lead to stabilizer

molecules precipitating out of solution as a polymerization progresses. Experimental results suggest that particle formation is complete very soon after a polymerization commences (before 0.1% conversion of monomer<sup>33</sup>). Therefore, at nucleation, the majority of the monomer will remain in the continuous phase and during this stage the accessibility of stabilizer molecules is very important. The solubility results reported here mimic the conditions under which nucleation and initial particle stabilization take place. In the future, it might be interesting to profile how stabilizer solubility changes with reducing monomer concentration; this may influence the ability of the stabilizer to continue to extend into the CO<sub>2</sub> phase throughout the reaction. Information of this nature would further elucidate the trends in stabilizer ability observed for the different PFPE-*b*-PMMA stabilizers.

**Effect of PFPE-*b*-PMMA Concentration.** Stabilizers PFPE(1750)-*b*-PMMA(2000) and PFPE(1750)-*b*-PMMA(3300) were used to investigate the effect of stabilizer concentration on polymerization outcome (Table 4). Comparing entries 1 and 2, doubling the concentration of PFPE(1750)-*b*-PMMA(2000) led to a small improvement in product molecular weight and PDI. The particles obtained were found to be smaller in size and this is consistent with previous reports in



the literature.<sup>28,29,37</sup> A more dramatic effect was observed for the stabilizer PFPE(1750)-*b*-PMMA(3300). Increasing its concentration from 0.020 to 0.039 mol % significantly improved product molecular weight (Table 4, entries 3 and 4) and morphology (Figure 9, parts a and b); the PMMA product changed from a sticky, colorless solid to a white powder consisting of uniform, discrete particles. As a result of the reduced solubility of PFPE(1750)-*b*-PMMA(3300) compared to PFPE(1750)-*b*-PMMA(2000), it is likely that a greater concentration of PFPE(1750)-*b*-PMMA(3300) is required for there to be sufficient stabilizer molecules present in the continuous phase for effective stabilization. Surprisingly, increasing the concentration of PFPE(1750)-*b*-PMMA(3300) further to 0.078 mol % (entry 5) was found to have little effect on product particle size and particle size distribution. This may be a result of the continuous phase reaching saturation point, above which no further stabilizer is dissolved despite an increase in stabilizer concentration.

#### 4. Conclusion

We demonstrate that a range of stabilizers based upon a PFPE can be prepared with varying anchor group functionality for the dispersion polymerization of MMA in scCO<sub>2</sub>. The most active stabilizer was found to be a PFPE-*b*-PMMA diblock copolymer. A range of these copolymers were synthesized by ATRP from a PFPE-bromoester macroinitiator, which allowed the length of the PMMA block to be controlled. In addition, three different molecular weight PFPE chains were used as the macroinitiator species and this enabled the relative ratio of the PFPE and PMMA blocks to be manipulated. By this method we were able to investigate the effect of ASB on the ability of the PFPE-*b*-PMMA copolymers to stabilize dispersion polymerizations of MMA. Results suggest that for a PMMA anchor block of 2000 g/mol, the optimum CO<sub>2</sub>-philic portion is a PFPE chain with a molecular weight of 1750 g/mol (ASB = 1.1). This stabilizer led to high molecular weight PMMA in excellent yield with a very fine particle morphology. Increasing the length of the PMMA anchor block from 2000 to 5600 g/mol was found to reduce the molecular weight of the PMMA product and led to some aggregation of the polymer particles. These results highlight the importance of balance between the polymer-philic and CO<sub>2</sub>-philic portions within a stabilizer; if one portion is increased at the expense of the other a reduction in stabilizer efficiency results. Finally, cloud point measurements for the different stabilizers in CO<sub>2</sub> and a mixture of CO<sub>2</sub>/MMA provide some insight into the solubility requirements for a good stabilizer. Most importantly, the stabilizer does not have to be completely soluble in pure CO<sub>2</sub> but should be dispersed throughout the initial CO<sub>2</sub>/MMA reaction mixture with the aid of MMA as a cosolvent.

**Acknowledgment.** We thank Mr. P. A. Fields and Mr. R. G. M. Wilson for technical help and Dr. W. Wang for his help and advice. We also thank Uniqema and EPSRC for funding a studentship (H.M.W.), and EPSRC for funding a fellowship (C.N.). S.M.H. is a Royal Society Wolfson Research Merit Award Holder.

#### References and Notes

- McHugh, M. A.; Krukonis, V. J. *Supercritical fluid extraction: principles and practice*, 2nd ed.; Butterworth-Heinemann: Stoneham, U.K., 1993.
- Leitner, W. *Nature (London)* **2000**, *405*, 129–130.
- Woods, H. M.; Silva, M. M. C. G.; Nouvel, C.; Shakesheff, K. M.; Howdle, S. M. *J. Mater. Chem.* **2004**, *14*, 1663–1678.
- Cooper, A. I. *J. Mater. Chem.* **2000**, *10*, 207–234.
- Kendall, J. L.; Canelas, D. A.; Young, J. L.; DeSimone, J. M. *Chem. Rev.* **1999**, *99*, 543–563.
- Cooper, A. I. *Adv. Mater.* **2001**, *13*, 1111–1114.
- Kazarian, S. G. *Polym. Sci.* **2000**, *42*, 78–101.
- Jessop, P. G.; Ikariya, T.; Noyori, R. *Science* **1995**, *269*, 1065–1069.
- Baiker, A. *Chem. Rev.* **1999**, *99*, 453–473.
- Taylor, L. T. *Supercritical fluid extraction*; Wiley: New York, 1996.
- Adasoglu, N.; Dincer, S.; Bolat, E. *J. Supercrit. Fluids* **1994**, *7*, 93–99.
- Hanrahan, J. P.; Ziegler, K. J.; Glennon, J. D.; Steytler, D. C.; Eastoe, J.; Dupont, A.; Holmes, J. D. *Langmuir* **2003**, *19*, 3145–3150.
- Kirby, C. F.; McHugh, M. A. *Chem. Rev.* **1999**, *99*, 565–602.
- Rindfleisch, F.; DiNoia, T. P.; McHugh, M. A. *J. Phys. Chem.* **1996**, *100*, 15581–15587.
- Taylor, D. K.; Keiper, J. S.; DeSimone, J. M. *Ind. Eng. Chem. Res.* **2002**, *41*, 4451–4459.
- Howdle, S. M. *Green Chem.* **2002**, *4*, G29–G31.
- Yu, K. M. K.; Steele, A. M.; Zhu, J.; Fu, Q. J.; Tsang, S. C. J. *Mater. Chem.* **2003**, *13*, 130–134.
- Johnston, K. P.; Cho, D. M.; DaRocha, S. R. P.; Psathas, P. A.; Ryoo, W.; Webber, S. E.; Eastoe, J.; Dupont, A.; Steytler, D. C. *Langmuir* **2001**, *17*, 7191–7193.
- Liu, H. W.; Yates, M. Z. *Langmuir* **2003**, *19*, 1106–1113.
- Desimone, J. M.; Maury, E. E.; Menciloglu, Y. Z.; McClain, J. B.; Romack, T. J.; Combes, J. R. *Science* **1994**, *265*, 356–359.
- Hsiao, Y. L.; Maury, E. E.; Desimone, J. M.; Mawson, S.; Johnston, K. P. *Macromolecules* **1995**, *28*, 8159–8166.
- Hems, W. P.; Yong, T. M.; van Nunen, J. L. M.; Cooper, A. I.; Holmes, A. B.; Griffin, D. A. *J. Mater. Chem.* **1999**, *9*, 1403–1407.
- Giles, M. R.; Griffiths, R. M. T.; Aguiar-Ricardo, A.; Silva, M. M. C. G.; Howdle, S. M. *Macromolecules* **2001**, *34*, 20–25.
- Johnston, K. P. *Curr. Opin. Colloid Interface Sci.* **2000**, *5*, 351–356.
- Canelas, D. A.; DeSimone, J. M. *Macromolecules* **1997**, *30*, 5673–5682.
- Yong, T. M.; Hems, W. P.; vanNunen, J. L. M.; Holmes, A. B.; Steinke, J. H. G.; Taylor, P. L.; Segal, J. A.; Griffin, D. A. *Chem. Commun.* **1997**, 1811–1812.
- Shiho, H.; DeSimone, J. M. *J. Polym. Sci., Polym. Chem.* **2000**, *38*, 3783–3790.
- Canelas, D. A.; Betts, D. E.; DeSimone, J. M. *Macromolecules* **1996**, *29*, 2818–2821.
- Lepilleur, C.; Beckman, E. J. *Macromolecules* **1997**, *30*, 745–756.
- Canelas, D. A.; Betts, D. E.; DeSimone, J. M. *Polym. Prepr. (Div. Polym. Chem., Am. Chem. Soc.)* **1997**, *38*, 628–629.
- Li, G.; Yates, M. Z.; Johnston, K. P.; Howdle, S. M. *Macromolecules* **2000**, *33*, 4008–4014.
- O'Neill, M. L.; Yates, M. Z.; Johnston, K. P.; Smith, C. D.; Wilkinson, S. P. *Macromolecules* **1998**, *31*, 2838–2847.
- O'Neill, M. L.; Yates, M. Z.; Johnston, K. P.; Smith, C. D.; Wilkinson, S. P. *Macromolecules* **1998**, *31*, 2848–2856.
- Wang, W. X.; Griffiths, R. M. T.; Naylor, A.; Giles, M. R.; Irvine, D. J.; Howdle, S. M. *Polymer* **2002**, *43*, 6653–6659.
- Wang, W. X.; Giles, M. R.; Bratton, D.; Irvine, D. J.; Armes, S. P.; Weaver, J. V. W.; Howdle, S. M. *Polymer* **2003**, *44*, 3803–3809.
- Giles, M. R.; Hay, J. N.; Howdle, S. M.; Winder, R. J. *Polymer* **2000**, *41*, 6715–6721.
- Christian, P.; Giles, M. R.; Griffiths, R. M. T.; Irvine, D. J.; Major, R. C.; Howdle, S. M. *Macromolecules* **2000**, *33*, 9222–9227.
- Christian, P.; Howdle, S. M.; Irvine, D. J. *Macromolecules* **2000**, *33*, 237–239.
- Wang, W.; Naylor, A.; Howdle, S. M. *Macromolecules* **2003**, *36*, 5424–5427.
- Licence, P.; Dellar, M. P.; Wilson, R. G. M.; Fields, P. A.; Litchfield, D.; Woods, H. M.; Howdle, S. M.; Poliakoff, M. *Rev. Sci. Instrum.* **2004**, *75*, 3233–3236.
- Cooper, A. I.; Hems, W. P.; Holmes, A. B. *Macromolecules* **1999**, *32*, 2156–2166.



- (42) Furno, F.; Licence, P.; Howdle, S. M.; Poliakoff, M. *Act. Chim.* **2003**, 62–66.
- (43) Rosell, A.; Storti, G.; Morbidelli, M.; Bratton, D.; Howdle, S. M. *Macromolecules* **2004**, 37, 2996–3004.
- (44) Matyjaszewski, K.; Pattern, T. E.; Xia, J. *J. Am. Chem. Soc.* **1997**, 119, 674–680.
- (45) O'Neill, M. L.; Cao, Q.; Fang, R.; Johnston, K. P.; Wilkinson, S. P.; Smith, C. D.; Kerschner, J. L.; Jureller, S. H. *Ind. Eng. Chem. Res.* **1998**, 37, 3067–3079.
- (46) Barrett, K. E. J. *Dispersion Polymerisation in Organic Media*; New York, 1975.
- (47) Lora, M.; McHugh, M. A. *Fluid Phase Equilib.* **1999**, 157, 285–297.
- (48) Fehrenbacher, U.; Ballauff, M. *Macromolecules* **2002**, 35, 3653–3661.
- (49) Lepilleur, C.; Beckman, E. J.; Schonemann, H.; Krukonis, V. *J. Fluid Phase Equilib.* **1997**, 134, 285–305.

MA048406+